

## Gas Phase, Solution, and Solid State Alkali Ion Binding by the $[\text{NbE}_8]^{3-}$ ( $\text{E} = \text{As}, \text{Sb}$ ) Complexes: Synthesis, Structure, and Spectroscopy

Banu Kesanli,<sup>†</sup> James Fettinger,<sup>†</sup> Brian Scott,<sup>‡</sup> and Bryan Eichhorn<sup>\*†</sup>

Department of Chemistry and Biochemistry, University of Maryland, College Park, Maryland 20742 and Chemical Science and Technology Divisions, Los Alamos National Laboratory, Los Alamos, New Mexico 87545

Received December 4, 2003

Toluene solutions of  $\text{Nb}(\text{toluene})_2$  react with ethylenediamine solutions of  $\text{K}_3\text{E}_7$  ( $\text{E} = \text{As}, \text{Sb}$ ) in the presence of 2,2,2-crypt to give  $[\text{NbAs}_8]^{3-}$  (**2**) and  $[\text{NbSb}_8]^{3-}$  (**3**) ions, respectively, in low yields. The  $^{133}\text{Cs}$  NMR spectroscopy, ESIMS results (negative ion mode), and single-crystal X-ray structures of the ions are reported. The complexes have  $\text{S}_8$ -like  $\text{E}_8$  rings with Nb atoms in the center. The 1:1 complex of **2** with  $\text{Cs}^+$  was observed in solution and also in the gas phase as the oxidized ion  $[\text{CsNbAs}_8]^{1-}$ . The anion **2** selectively binds to  $\text{Cs}^+$  in solution even in the presence of excess  $\text{Na}^+$ . Other gas-phase ions formed include  $[\text{Cs}_2(\text{NbAs}_8)]^{1-}$ ,  $[\text{KCs}(\text{NbAs}_8)]^{1-}$ ,  $[\text{KCs}(\text{NbAs}_8)_2]^{1-}$ ,  $[\text{KNbAs}_8]^{1-}$ , and  $[\text{K}_2\text{NbAs}_8]^{1-}$ .

The sequestration and transport of alkali ions by organic and bio-molecules<sup>1–4</sup> has been studied extensively in the past several years due to the importance of alkalis in chemistry and biology. One important application of sequestering agents is the removal of the dangerous radionuclide  $^{137}\text{Cs}$  from nuclear waste.<sup>5,6</sup> Other alkali ions,  $\text{Na}^+$  and  $\text{K}^+$ , are also found in nuclear waste streams and are in higher concentrations than  $^{137}\text{Cs}^+$ . Therefore, it is desirable to develop a method that selectively binds  $\text{Cs}^+$  in the presence of other ions. Various methods have been explored to achieve selectivity, which include use of calixarenes and their derivatives<sup>7</sup> and macrocyclic ligands<sup>2,8–10</sup> such as crown ethers and cryptands.<sup>11–13</sup> Self-assembled ionophores with high  $\text{Cs}^+$

selectivity are also promising in designing ionophores for  $^{137}\text{Cs}$  remediation.<sup>4,14–17</sup>

There are many inorganic materials that bind alkali metal ions as well,<sup>18</sup> however, those that selectively bind specific ions such as cesium or rubidium are less common. Recently, tailored inorganic hosts, such as the cyanometalate box-like cages reported by Rauchfuss et al.,<sup>19–21</sup> have shown great potential for selective alkali ion sequestration. Another group of “inorganic ligands” that showed selectivity for binding large alkali ions are the  $[\text{ME}_8]^{n-}$  type complexes where  $\text{M} = \text{Cr}, \text{Mo}$ ;  $\text{E} = \text{As}, \text{Sb}$ ; and  $n = 2, 3$ .<sup>22–24</sup> von Schnering

\* E-mail: eichhorn@umd.edu.

<sup>†</sup> University of Maryland.

<sup>‡</sup> Los Alamos National Laboratory.

- (1) Bradshaw, J. S.; Izatt, R. M. *Acc. Chem. Res.* **1997**, *30*, 338.
- (2) Krakowiak, K. E.; Bradshaw, J. S.; Zhu, C. Y.; Hathaway, J. K.; Dalley, N. K.; Izatt, R. M. *J. Org. Chem.* **1994**, *59*, 4082.
- (3) Assmus, R.; Bohmer, V.; Harrowfield, J. M.; Ogden, M. I.; Richmond, W. R.; Skelton, B. W.; White, A. H. *J. Chem. Soc., Dalton Trans.* **1993**, 2427.
- (4) Wong, A.; Fettinger, J. C.; Forman, S. L.; Davis, J. T.; Wu, G. *J. Am. Chem. Soc.* **2002**, *124*, 742.
- (5) Schulz, W. W.; Bray, L. A. *Sep. Sci. Technol.* **1987**, *22*, 191.
- (6) Nash, K. L.; Barrans, R. E.; Chiarizia, R.; Dietz, M. L.; Jensen, M. P.; Rickert, P. G.; Moyer, B. A.; Bonnesen, P. V.; Bryan, J. C.; Sachleben, R. A. *Solvent Extr. Ion Exch.* **2000**, *18*, 605.
- (7) Ungaro, R.; Casnati, A.; Ugozzoli, F.; Pochini, A.; Dozol, J. F.; Hill, C.; Rouquette, H. *Angew. Chem., Int. Ed. Engl.* **1994**, *33*, 1506.
- (8) McDowell, W. J.; Case, G. N.; McDonough, J. A.; Bartsch, R. A. *Anal. Chem.* **1992**, *64*, 3013.
- (9) Deng, Y. P.; Sachleben, R. A.; Moyer, B. A. *J. Chem. Soc., Faraday Trans.* **1995**, *91*, 4215.

- (10) Bryant, J. A.; Ho, S. P.; Knobler, C. B.; Cram, D. J. *J. Am. Chem. Soc.* **1990**, *112*, 5837.
- (11) Meier, U. C.; Detellier, C. *J. Phys. Chem. A* **1999**, *103*, 3825.
- (12) Meier, U.; Detellier, C. *J. Phys. Chem. A* **1998**, *102*, 1888.
- (13) Mei, E.; Popov, A. I.; Dye, J. L. *J. Am. Chem. Soc.* **1977**, *99*, 6532.
- (14) Davis, J. T. *Angew. Chem., Int. Ed.* **2004**, in press.
- (15) Shi, X.; Fettinger, J. C.; Davis, J. T. *Angew. Chem., Int. Ed.* **2001**, *40*, 2827.
- (16) Shi, X. D.; Fettinger, J. C.; Cai, M. M.; Davis, J. T. *Angew. Chem., Int. Ed.* **2000**, *39*, 3124.
- (17) Cai, M.; Marlow, A. L.; Fettinger, J. C.; Fabris, D.; Haverlock, T. J.; Moyer, B. A.; Davis, J. T. *Angew. Chem., Int. Ed.* **2000**, *39*, 1283.
- (18) Wells, A. F. *Structural Inorganic Chemistry*, 5th ed.; Oxford University Press: New York, 1991.
- (19) Kuhlman, M. L.; Rauchfuss, T. B. *J. Am. Chem. Soc.* **2003**, *125*, 10084.
- (20) Hsu, S. C. N.; Ramesh, M.; Espenson, J. H.; Rauchfuss, T. B. *Angew. Chem., Int. Ed.* **2003**, *42*, 2663.
- (21) Contakes, S. M.; Kuhlman, M. L.; Ramesh, M.; Wilson, S. R.; Rauchfuss, T. B. *Proc. Nat. Acad. Sci.* **2002**, *99*, 4889.
- (22) von Schnering, H. G.; Wolf, J.; Weber, D.; Ramirez, R.; Meyer, T. *Angew. Chem., Int. Ed. Engl.* **1986**, *25*, 353.
- (23) Eichhorn, B. W.; Matamanna, S. P.; Gardner, D. R.; Fettinger, J. C. *J. Am. Chem. Soc.* **1998**, *120*, 9708.

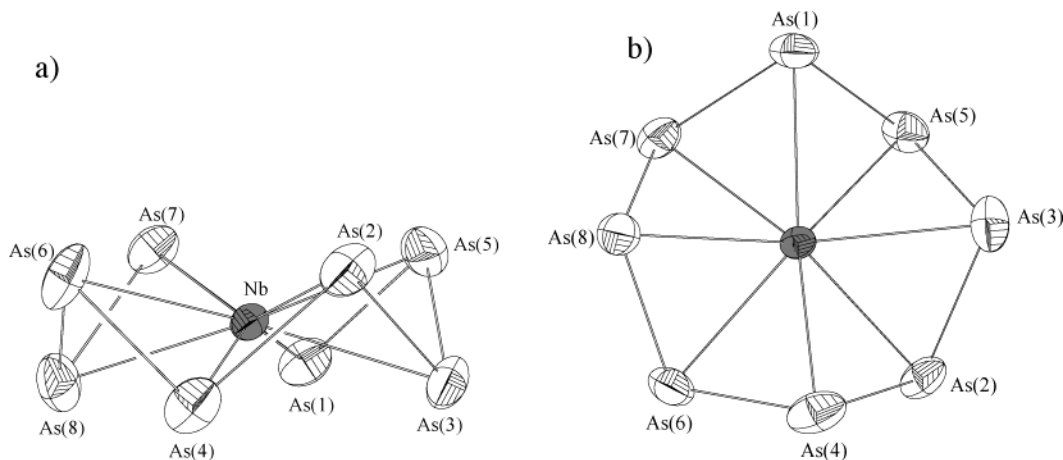
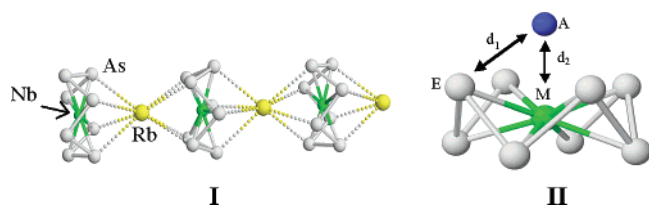


**Figure 1.** Thermal ellipsoid plot of  $[\text{NbAs}_8]^{3-}$  ion: (a) side view, and (b) top view.

and co-workers<sup>22</sup> described the first member in this class of complexes with the characterization of the  $[\text{RbNbAs}_8]^{2-}$  anion (**1**). This polymeric anion contains  $[\text{NbAs}_8]^{3-}$  crown-like subunits that bind to  $\text{Rb}^+$  ions in a one-dimensional chain structure (see I below). Subsequently, we described<sup>23</sup> the complex  $[\text{MoAs}_8]^{2-}$  that is isostructural and isoelectronic to the  $[\text{NbAs}_8]^{3-}$  subunit of **1**. Unlike von Schnering's complex, the  $[\text{MoAs}_8]^{2-}$  ion is not coordinated to any alkali ions and exists as a "free ion" in the crystal lattice. In both complexes, the  $\text{As}_8$  rings have crown-like  $S_8$  structures with eight-coordinate metal atoms in the center. The coordination geometry of the centered transition metal can be viewed as a highly compressed square antiprism. In contrast, the rubidium ion in **1** is in a highly elongated square-antiprismatic environment. The remaining two  $[\text{Rb}(2,2,2\text{-crypt})]^+$  counterions in **1** and the  $[\text{K}(2,2,2\text{-crypt})]^+$  counterions in the  $[\text{K}(2,2,2\text{-crypt})]_2[\text{MoAs}_8]$  salt are well separated from their respective anions.



The degree of aggregation in the general series of the  $[\text{ME}_8]^{n-}$  type complexes where  $M = \text{Cr}, \text{Mo}$ ;  $E = \text{As}, \text{Sb}$ ; and  $n = 2, 3$  depends on the size of the pnictide atom ( $E$ ), the transition metal atom ( $M$ ), and the alkali ion.<sup>24</sup> The interactions between the ring and the cations are shown in II above. The distance  $d_2$  is the separation between the alkali ion and the central metal atom, and  $d_1$  is the bond distance between the  $\text{E}_8$  ring and the alkali ion. Chain formation occurs when favorable  $A-E$  bond distances can be achieved (optimal  $d_1$ ) while keeping the  $M \cdots A$  Coulombic repulsions at a minimum (long  $d_2$ ). As the  $\text{ME}_8$  unit becomes larger, a larger alkali ion is needed to satisfy the requirements for chain formation. Alkali ions that are too small relative to the ring must drop down into the  $\text{E}_8$  cavity to optimize the  $A-E$  bond distance, which generates a destabilizing  $d_1$

separation. In this case, a free ion structure is formed. For example,  $\text{K}^+$  forms a 1D chain with the  $[\text{CrAs}_8]^{3-}$  ion whereas the smaller  $\text{Na}^+$  forms a free ion structure. Because solid state and gas-phase chemistry often differ from solution chemistry (the phase of relevance), we embarked on a comparative binding study of the  $[\text{NbAs}_8]^{3-}$  ion. Described here is the synthesis and characterization of the free ion  $[\text{NbAs}_8]^{3-}$  and its Sb analogue,  $[\text{NbSb}_8]^{3-}$ . In this study, we compare and contrast the  $\text{Cs}^+$  ion binding of  $[\text{NbAs}_8]^{3-}$  in the solid state, solution, and the gas phase by employing X-ray crystallography,  $^{133}\text{Cs}$  NMR spectroscopy, and electrospray mass spectrometry (ESIMS), respectively. The interplay between  $A-E$  bonding and  $A \cdots M$  Coulombic repulsions in the solid state, solution, and the gas phase are described.

## Results

**Synthesis.** Toluene solutions of  $\text{Nb}(\text{toluene})_2$  react with ethylenediamine (en) solutions of  $\text{K}_3\text{E}_7$  ( $E = \text{As}, \text{Sb}$ ) in the presence of 3 equiv of 2,2,2-crypt to give  $[\text{K}(2,2,2\text{-crypt})]^+$  salts of  $[\text{NbAs}_8]^{3-}$  (**2**) and  $[\text{NbSb}_8]^{3-}$  (**3**) ions, respectively, in low crystalline yields. These reactions do not occur in the absence of 2,2,2-crypt. Similar 2,2,2-crypt initiated reactions have been observed in the synthesis of other metalated Zintl ions.<sup>23,25</sup> The title complexes have been characterized by  $^{133}\text{Cs}$  NMR, ESIMS, and single-crystal X-ray diffraction. Both salts are red in the solid state, decompose upon exposure to air, and are soluble in DMF and  $\text{CH}_3\text{CN}$ . The actual mechanism of the formation of the  $[\text{NbE}_8]^{3-}$  ions from the parent  $\text{E}_7^{3-}$  ions is not clear at present.

**Solid State Structures.** The  $[\text{K}(2,2,2\text{-crypt})]^+$  salts of **2** and **3** are monoclinic and have  $P2_1/n$  and  $I2/a$  crystal symmetries, respectively. An ORTEP drawing of the  $[\text{NbAs}_8]^{3-}$  ion (**2**) is given in Figure 1 as a representative of the  $[\text{NbE}_8]^{3-}$  structure type. A summary of the crystallographic data is given in Table 1, and the selected bond distances and angles for **2** are given in Table 2. The crystals of **3** diffracted very

(24) Kesanli, B.; Fettingner, J.; Eichhorn, B. *J. Am. Chem. Soc.* **2003**, *125*, 7367.

(25) Kesanli, B.; Fettingner, J.; Gardner, D. R.; Eichhorn, B. *J. Am. Chem. Soc.* **2002**, *124*, 4779.

**Table 1.** Crystallographic Data for the  $[\text{NbAs}_8]^{3-}$  and  $[\text{NbSb}_8]^{3-}$  Ions

compound	$[\text{K}(2,2,2\text{-crypt})]_3[\text{NbAs}_8]\cdot\text{en}$	$[\text{K}(2,2,2\text{-crypt})]_3[\text{NbSb}_8]$
empirical formula	$\text{C}_{56}\text{H}_{116}\text{As}_8\text{K}_3\text{N}_8\text{O}_{18}\text{Nb}$	$\text{C}_{162}\text{H}_{324}\text{Sb}_{24}\text{K}_9\text{N}_{18}\text{O}_{54}\text{Nb}_3$
formula weight	1999.14	6941.02
temp	193(2) K	193(2)
wavelength	0.71073 Å	0.71073
space group	$P2_1/n$	$I2/a$
unit cell dimensions		
<i>a</i> [Å]	18.243(4)	26.0588(9)
<i>b</i> [Å]	23.090(4)	25.3583(8)
<i>c</i> [Å]	19.265(4)	38.0508(17)
$\alpha$ [°]	90.0	90
$\beta$ [°]	91.01(1)	92.3650(10)
$\gamma$ [°]	90.0	90
volume (Å <sup>3</sup> )	8114(3)	25122.8(16)
Z	4	4
density [g/cm <sup>3</sup> ]	1.63	1.835
abs coeff [mm <sup>-1</sup> ]	3.604	2.877
GOF on $F^2$	1.005	2.003
final R [ $I > 2\sigma(I)$ ] <sup>a</sup>		
R1	0.0509	0.0940
wR2	0.0903 [6310 Data]	0.2561
R indices (all data) <sup>a</sup>		
R1	0.1138	0.1286
wR2	0.1098	0.2918

<sup>a</sup> The function minimized during the full-matrix least-squares refinement was  $\sum w(F_o^2 - F_c^2)$  where  $w = 1/[\sigma^2(F_o^2) + (0.0180 * P)^2 + 10.4114 * P]$  and  $P = (\max(F_o^2, 0) + 2 * F_c^2) / 3$ .

**Table 2.** Selected Distances (Å) and Angles (°) for the  $[\text{NbAs}_8]^{3-}$  Ion

distances		
Nb–As(1)	2.634(1)	As(1)–As(5) 2.445(2)
Nb–As(2)	2.624(1)	As(1)–As(7) 2.450(2)
Nb–As(3)	2.616(1)	As(2)–As(3) 2.444(2)
Nb–As(4)	2.627(1)	As(2)–As(4) 2.450(2)
Nb–As(5)	2.637(1)	As(3)–As(5) 2.440(1)
Nb–As(6)	2.635(1)	As(4)–As(6) 2.453(1)
Nb–As(7)	2.614(1)	As(6)–As(8) 2.443(1)
Nb–As(8)	2.630(1)	As(7)–As(8) 2.447(2)
angles		
As(5)–As(1)–As(7)		92.01(5)
As(3)–As(2)–As(4)		93.26(5)
As(5)–As(3)–As(2)		94.25(5)
As(2)–As(4)–As(6)		92.55(5)
As(3)–As(5)–As(1)		92.68(5)
As(8)–As(6)–As(4)		93.48(5)
As(8)–As(7)–As(1)		94.12(5)
As(6)–As(8)–As(7)		94.42(5)

weakly, therefore the structure is of low quality. The  $[\text{K}(2,2,2\text{-crypt})]$  salt of **3** is isomorphic to the previously reported  $[\text{K}(2,2,2\text{-crypt})]_3[\text{MoSb}_8]$  salt, but, due to the low quality of the refinement, the details of the metric parameters will not be discussed herein. However, the bond distances and angles fall into the range for the expected values for  $[\text{NbSb}_8]^{3-}$  complex. The salt of **2** contains one en solvate molecule, whereas **3** is solvate-free.

The  $[\text{NbE}_8]^{3-}$  complexes (E = As, Sb) are similar to the Mo analogues<sup>23,24</sup>  $[\text{MoAs}_8]^{2-}$  and  $[\text{MoSb}_8]^{3-}$ , with crown-like  $E_8$  structures, interstitial Nb atoms, and overall  $D_{4d}$  point symmetry. A summary of the metric parameters for this class of  $\text{ME}_8^{n-}$  clusters is given in Table 3. The  $[\text{NbE}_8]^{3-}$  complexes exist as “free ions” that are well separated from the  $[\text{K}(2,2,2\text{-crypt})]^+$  cations, in contrast to the 1D chain complex,  $[\text{RbNbAs}_8]^{2-}$ , where the alkali ions are involved in chain formation.<sup>22</sup> The bond distances and angles for **2** are virtually identical to those of **1**. A similar situation is observed for the free ion  $[\text{CrAs}_8]^{3-}$  and its 1D chain complex  $[\text{KCrAs}_8]^{2-}$ .<sup>24</sup>

**Table 3.** Average Bond Distances (Å) and Angles (deg) for the  $\text{ME}_8^{n-}$  Ions

$[\text{NbE}_8]^{3-}$	M–E	E–E	E–E–E(°)	ref.
$[\text{NbAs}_8]^{3-}$	2.627(2)	2.446(2)	93.35(5)	this work
$[\text{RbNbAs}_8]^{2-}$	2.62	2.434	93.7	ref 22
$[\text{NbSb}_8]^{3-}$	2.85(1)	2.78(1)	86.5(2)	this work <sup>a</sup>
$[\text{KCrAs}_8]^{2-}$	2.532(6)	2.418(7)	89.50(3)	ref 24
$[\text{CrAs}_8]^{3-}$	2.540(5)	2.426(5)	89.54(16)	ref 24
$[\text{MoAs}_8]^{2-}$	2.567(2)	2.429(2)	90.60(6)	ref 23
$[\text{MoSb}_8]^{3-}$	2.825(2)	2.786(2)	85.05(4)	ref 24

<sup>a</sup> Low-quality structural refinement, see Experimental Section for details.

The average E–E bond distances for **1** and **2** (2.4464(14) Å and 2.782(5) Å, respectively) are ca. 0.34 Å shorter than those of **3** and  $[\text{MoSb}_8]^{3-}$  (see Table 3). This difference is less than expected on the basis of the 0.25 Å difference of covalent radii of the elements, but only slightly less than the 0.38 Å difference in related isostructural complexes.<sup>26</sup> In contrast, the M–E distances increase by 0.22–0.25 Å when comparing As<sub>8</sub> to Sb<sub>8</sub> complexes with the same metals. The larger apparent change in the Mo series may be due in part to the change in formal oxidation states of the metals in the  $[\text{MoAs}_8]^{2-}$  and  $[\text{MoSb}_8]^{3-}$  pair. The average E–E–E bond angles in the As<sub>8</sub> and the Sb<sub>8</sub> complexes vary to accommodate the different transition metals (see discussion).

**Mass Spectrometry.** The ESIMS studies of the  $[\text{K}(2,2,2\text{-crypt})]_3[\text{NbAs}_8]$  salt (DMF solution, negative ion mode) show the oxidized molecular ion  $[\text{NbAs}_8]^{1-}$  and the K<sup>+</sup> coordinated species  $[\text{KNbAs}_8]^{1-}$ ,  $[\text{K}_2\text{NbAs}_8]^{1-}$ , and  $[\text{K}(\text{NbAs}_8)_2]^{1-}$ . Various naked As clusters and their Nb complexes are also present in the spectrum, which include the commonly observed<sup>23,29</sup> nine-atom cluster, As<sub>9</sub>, coordinated to K<sup>+</sup> and Nb to form the  $[\text{KNbAs}_9]^{1-}$  ion. The K<sup>+</sup> ions in the MS studies presumably originate from the  $[\text{K}(2,2,2\text{-crypt})]^+$  ions. Structures of the proposed complexes will be discussed later.

In the presence of CsBPh<sub>4</sub>, the  $[\text{K}(2,2,2\text{-crypt})]_3[\text{NbAs}_8]$  ESIMS spectra (CH<sub>3</sub>CN solution, negative ion mode) show the same K<sup>+</sup> coordinated complexes as well as Cs<sup>+</sup> and Cs<sup>+</sup>/K<sup>+</sup> mixed ion clusters (Figure 2). These include the 1:1 complex  $[\text{CsNbAs}_8]^{1-}$ , the 2:1 complex  $[\text{Cs}_2\text{NbAs}_8]^{1-}$ , the mixed 2:1 complex  $[\text{KCsNbAs}_8]^{1-}$ , and the 2:2  $[\text{KCs}(\text{NbAs}_8)_2]^{1-}$  complexes. The protonated analogues of these ions are also present. Alkali ion extraction from 2,2,2-crypt in the gas phase has been observed in the mass spectral studies of other Zintl ion transition metal complexes as well as the naked Group 14 and 15 Zintl ions.<sup>25,27</sup>

During the gas-phase studies of **2**, new peaks appear with time and are most likely the decomposition products of **2**. These ions include the K<sup>+</sup> coordinated 10-atom cluster  $[\text{KAs}_{10}]^{1-}$  and its Nb complexes,  $[\text{NbAs}_{10}]^{1-}$  and  $[\text{K}_2\text{NbAs}_{10}]^{1-}$ . The  $[\text{K}_2\text{NbAs}_{10}]^{1-}$  ion is the potassium salt of  $\text{NbAs}_{10}^{3-}$ , which may be the analogue of the recently

(26) Charles, S.; Bott, S. G.; Rheingold, A. L.; Eichhorn, B. W. *J. Am. Chem. Soc.* **1994**, *116*, 8077.

(27) Fassler, T. F.; Muhr, H. J.; Hunziker, M. *Eur. J. Inorg. Chem.* **1998**, 1433.

(28) Urnezus, E.; Brennessel, W. W.; Cramer, C. J.; Ellis, J. E.; Schleyer, P. V. *Science* **2002**, *295*, 832.

(29) Moses, M. J.; Fettingner, J.; Eichhorn, B. *J. Am. Chem. Soc.* **2002**, *124*, 5944.

## Structure of $[NbE_8]^{3-}$ ( $E = As, Sb$ ) Complexes

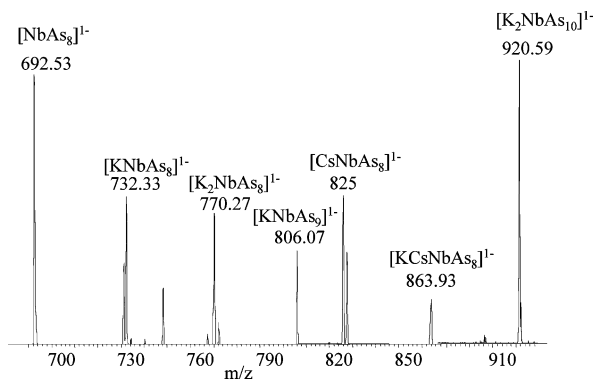


**Figure 2.** ESIMS of a mixture of  $CsPh_4B$  and  $[K(2,2,2-crypt)]_3[NbAs_8]$  recorded from a  $CH_3CN$  solution.

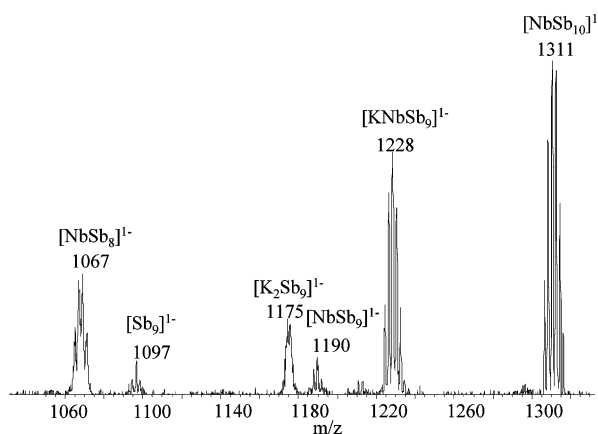
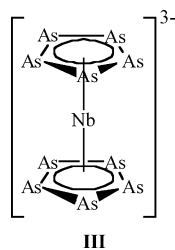


**Figure 3.** ESIMS of  $[K(2,2,2-crypt)]_3[NbSb_8]$  in DMF.

reported<sup>28</sup> carbon-free metallocene  $TiP_{10}^{2-}$ . The  $NbAs_{10}^{3-}$  ion would have an 18-electron Nb center in contrast to the 16-electron  $TiP_{10}^{2-}$ . The formation of  $E_5$  rings from polypnictide solutions has been observed previously in the synthesis of the  $[Pd_7As_{16}]^{4-}$ ,  $[Ni_5Sb_{17}]^{3-}$ , and  $[As@Ni_{12}@As_{20}]^{3-}$  ions.<sup>29–31</sup>



The ESI mass spectrum of the  $[K(2,2,2-crypt)]_3[NbSb_8]$  salt (DMF solutions, negative ion mode) shows the oxidized molecular  $[NbSb_8]^{1-}$  anion (Figure 3) together with naked Sb clusters such as the protonated  $[H_2Sb_8]^{1-}$ . In contrast to the mass spectrum of **2**, the  $K^+$  - coordinated molecular ion of **3** is not observed. This lack of coordination is consistent with expectations based on the previous studies on the Group 6 analogues (see II) in which “small” alkali metal ions do not form coordination complexes.<sup>24</sup>

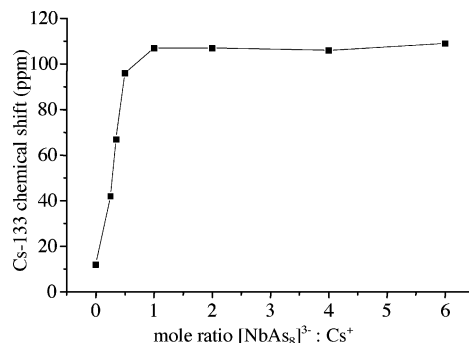


**Figure 4.** Plot of  $^{133}Cs$  chemical shift vs mole ratio of  $[NbAs_8]^{3-}$  to  $Cs^+$ .

The recurring<sup>23,29</sup> nine-atom byproduct  $[Sb_9]^{1-}$ , and its  $K^+$  and Nb derivatives,  $[K_2Sb_9]^{1-}$ ,  $[NbSb_9]^{1-}$ , and  $[KNbSb_9]^{1-}$  ions are present as well (Figure 3). The mass spectrum of **3** also shows an  $[NbSb_{10}]^{1-}$  ion, however,  $K^+$  coordination is not observed in this case and only the oxidized molecular ion has been detected. The structure of  $Sb_9^{3-}$  remains unknown.

**Solution Studies.**  $^{133}Cs$  NMR has found wide application in studying  $Cs^+$  ion binding and complexation in many compounds.  $^{133}Cs$  has a spin of 7/2 with a small quadrupole moment of  $-3 \times 10^{25} m^2$  and is 100% abundant.<sup>13,32</sup> This technique was employed to study the binding between  $Cs^+$  and  $[NbAs_8]^{3-}$  by titration experiments involving  $CH_3CN$  solutions of the respective ions. In the  $^{133}Cs$  NMR titration experiments, the  $Cs^+$  concentration was held constant at 1.0 mM and the  $^{133}Cs$  chemical shifts were recorded at different concentrations of the  $[NbAs_8]^{3-}$  ion (0.25, 0.35, 0.5, 1.0, 2.0, 4.0, and 6.0 mM, prepared from the  $[K(2,2,2-crypt)]_3[NbAs_8]$  salt). The plot of  $^{133}Cs$  chemical shifts vs molar ratio of  $[NbAs_8]^{3-}$  to  $Cs^+$  in  $CH_3CN$  is given in Figure 4. The  $CH_3CN$  solutions of  $CsBPh_4$  give sharp  $^{133}Cs$  NMR resonances at 12 ppm. Upon addition of **2**, the  $^{133}Cs$  signal systematically shifts downfield to a limiting value of 107 ppm, which corresponds to the 1:1 molar ratio of  $Cs^+$ :**2**. Beyond this point, addition of more  $[NbAs_8]^{3-}$  ion does not affect the chemical shift or line shape of the  $^{133}Cs$  resonance. These data suggest that the 1:1 complex  $[CsNbAs_8]^{2-}$  is favored in  $CH_3CN$  solutions over the 2:1 and 1:2 complexes. However, the presence of a 2:1 complex  $[Cs_2NbAs_8]^{1-}$  that is in fast exchange with the 1:1 complex and free  $Cs^+$  cannot be discounted on the basis of these data. There is a fast exchange between free  $Cs^+$  and complexed  $Cs^+$  on NMR time scale giving rise to an average chemical shift in all spectra.<sup>17</sup>

Because the use of 2,2,2-crypt is necessary to encapsulate the  $K^+$  ion in the synthesis of complex **2**, there are frequently trace amounts of free 2,2,2-crypt in the crystalline samples of **2**. Competition studies showed that  $Cs^+$  preferentially binds to free 2,2,2-crypt in the presence of **2**. To circumvent the problem of competitive binding in the titration experiments,  $NaPh_4B$  was added to each solution to sequester the free 2,2,2-crypt.  $Na^+$  does not bind to **2** (see below) and has a higher affinity for 2,2,2-crypt than does  $Cs^+$ . In a control

(30) Moses, M. J.; Fettinger, J. C.; Eichhorn, B. W. *Science* **2003**, *300*, 778.

(31) Moses, M. J.; Fettinger, J. C.; Eichhorn, B. W. To be submitted for publication.

(32) Drago, R. S. *Physical Methods for Chemists*, 2nd ed.; Saunders: New York, 1992.

experiment, 3 equiv of Na(2,2,2-crypt)BPh<sub>4</sub> were mixed with 1 equiv of CsBPh<sub>4</sub> in CH<sub>3</sub>CN and the <sup>133</sup>Cs NMR spectra were recorded. The <sup>133</sup>Cs chemical shift of the free Cs<sup>+</sup> was unaffected by the presence of [Na(2,2,2-crypt)]<sup>+</sup>. This result indicates that the equilibrium heavily favors Na<sup>+</sup>-crypt coordination and is consistent with literature studies.<sup>1</sup> Similar control experiments with [K(2,2,2-crypt)]<sup>+</sup> gave identical results. Dilution of the control experiments and the titration experiments did not affect the <sup>133</sup>Cs resonances or their chemical shifts. Addition of *excess* NaPh<sub>4</sub>B to the Cs<sup>+</sup>-2 titration experiments (i.e., in excess of the free 2,2,2-crypt concentration) also did not affect the <sup>133</sup>Cs NMR chemical shifts or line widths. These data show that Cs<sup>+</sup> binding to [NbAs<sub>8</sub>]<sup>3-</sup> is unaffected by the presence of Na<sup>+</sup> ions in solution. In addition, Cs<sup>+</sup> and Na<sup>+</sup> preferentially bind to [NbAs<sub>8</sub>]<sup>3-</sup> and 2,2,2-crypt, respectively, in solutions of host-guest mixtures.

## Discussion

von Schnering's original synthesis of the  ${}_{\infty}^1[\text{RbNbAs}_8]^{2-}$  1D chain complex involved the reduction of Nb<sub>2</sub>O<sub>5</sub> with the polyarsenide intermetallic RbAs in ethylenediamine solutions.<sup>22</sup> Importantly, their work showed that metal atoms could be stabilized in very unusual coordination geometries with polypnictide ligands and that the Zintl-Klemm formalism extends into the transition metal/Zintl ion complexes. von Schnering's synthetic route does not provide a general entry into ME<sub>8</sub><sup>n-</sup> chemistry (M = early transition metal; E = P, As, Sb; n = 2, 3), however, we have subsequently shown that a variety of ME<sub>8</sub><sup>n-</sup> ions are accessible through the use of labile, zerovalent M(arene)<sub>2</sub> precursors<sup>33</sup> with E<sub>7</sub><sup>3-</sup> ions.<sup>23,24</sup> Although the mechanism of formation in this reaction is unknown at present, the methodology seems to be generic even though the isolated yields are sometimes quite low. Repeated efforts to prepare a ZrE<sub>8</sub><sup>n-</sup> analogue from a Zr(naphthalene)<sub>3</sub><sup>2-</sup> precursor<sup>34</sup> and E<sub>7</sub><sup>3-</sup> solutions have been unsuccessful to date. We are continuing our attempted expansion of this unusual class of complexes.

The structure and bonding in the ME<sub>8</sub><sup>n-</sup> complexes has been of interest since von Schnering's original report<sup>22</sup> and is still a matter of current research.<sup>35</sup> In addition to the growing number of homoleptic ME<sub>8</sub><sup>n-</sup> ions, we have found examples of closely related centered 8-ring subunits, Pd(*cyclo*-Pd<sub>4</sub>As<sub>4</sub>) and Ni(*cyclo*-Ni<sub>4</sub>Sb<sub>4</sub>), in the clusters [Pd<sub>7</sub>As<sub>16</sub>]<sup>4-</sup> and [Ni<sub>5</sub>Sb<sub>18</sub>]<sup>4-</sup> respectively.<sup>29,31</sup> The E<sub>8</sub><sup>n-</sup> ligands demonstrate an unusual ability to stretch in an accordion-like fashion to accommodate larger or smaller transition metals. This versatility is best illustrated in the data in Table 3. In the five As<sub>8</sub> complexes reported, the M-As distances are adjusted to optimal bond lengths by compression or expansion of the As-As-As angles while keeping the As bond lengths essentially constant. In the series, the M-As distances differ by approximately 0.1 Å, whereas the average As-As distances are essentially the same with a variance

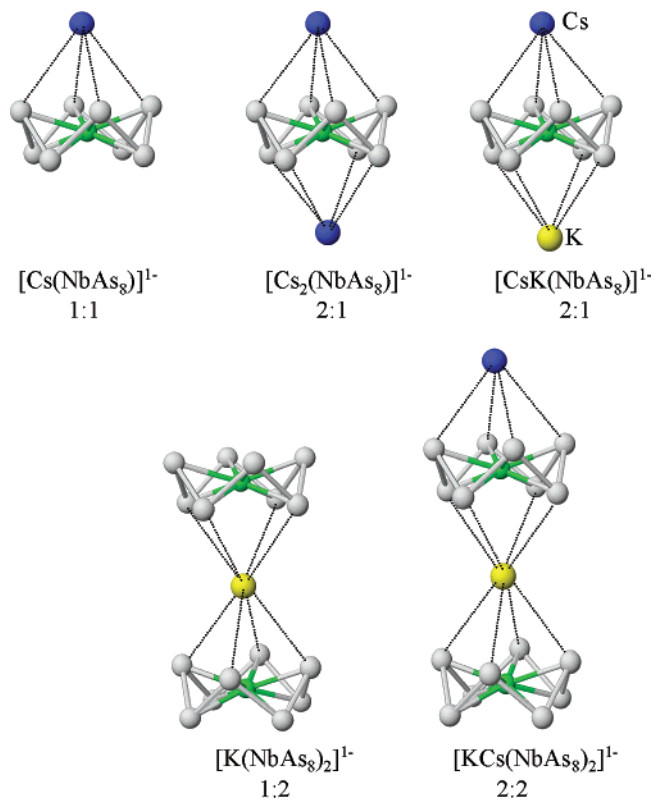


**Figure 5.** Proposed structures of some of the ions observed in the gas-phase studies of Cs<sup>+</sup> and [K(2,2,2-crypt)]<sub>3</sub>[NbAs<sub>8</sub>] in CH<sub>3</sub>CN. K is yellow, Cs is blue, Nb is green, and As is gray.

of less than ±0.03 Å. The As-As-As bond angles scale according to the metallic radii of the transition metals (Cr 1.30 Å, 1.36 Å, Nb 1.43 Å) and the M-E bond distances (Table 3).<sup>18</sup>

From this and previous studies, we have shown that [ME<sub>8</sub>]<sup>n-</sup> type ions selectively bind the larger alkali cations (Cs<sup>+</sup> and Rb<sup>+</sup>) in the presence of smaller alkalis (Na<sup>+</sup> and K<sup>+</sup>) in the solid state, solution, and (to a lesser extent) in the gas phase. In the solid state, crystals of the 1D chain complexes form from solution even when excess 2,2,2-crypt is present. The isolation of 1D chain complexes under these conditions does *not* imply that the relative alkali ion binding constant of the [ME<sub>8</sub>]<sup>n-</sup> ions is larger than that of 2,2,2-crypt. This phenomenon merely indicates that the effective concentration of free A<sup>+</sup> or A<sup>+</sup>-[ME<sub>8</sub>]<sup>n-</sup> complex is sufficient for favorable kinetics of crystallization of the chain structure. In fact, competitive binding experiments in solution show that all the alkali ions have a higher affinity for 2,2,2-crypt<sup>1</sup> and isoguanosine<sup>17</sup> than for the [ME<sub>8</sub>]<sup>n-</sup> ions under all conditions.

From the ESIMS studies of [MoAs<sub>8</sub>]<sup>2-</sup>, it was shown that [ME<sub>8</sub>]<sup>n-</sup> type ions selectively bind to larger alkali ions in the gas phase—even in the presence of the smaller alkalis.<sup>23</sup> In contrast, the gas-phase studies of **2** showed much less selectivity for Cs<sup>+</sup>, and different coordination complexes were observed. The proposed structures of some of the gas-phase species are given in Figure 5. Even though K<sup>+</sup> does not crystallize in the 1D chain structure with **2** in the solid state, it coordinates to **2** in the gas phase to give the [KNbAs<sub>8</sub>]<sup>1-</sup> and [K<sub>2</sub>NbAs<sub>8</sub>]<sup>1-</sup> complexes. The [K(NbAs<sub>8</sub>)]<sup>1-</sup>

(33) Pomije, M. K.; Kurth, C. J.; Ellis, J. E.; Barybin, M. V. *Organometallics* **1997**, *16*, 3582.

(34) Jang, M.; Ellis, J. E. *Angew. Chem., Int. Ed. Engl.* **1994**, *33*, 1973.

(35) Li, J.; Wu, K. C. *Inorg. Chem.* **2000**, *39*, 1538.

complex is observed as well, which is presumably a sandwich complex of **2**. Two new coordination assemblies are observed in the presence of  $\text{Cs}^+$ ; the 1:1 complex  $[\text{CsNbAs}_8]^{1-}$  together with the 2:1 complex  $[\text{Cs}_2(\text{NbAs}_8)]^{1-}$ . The former most likely has a single  $[\text{NbAs}_8]^{3-}$  ion capped by a  $\text{Cs}^+$  ion and the latter has two capping  $\text{Cs}^+$  ions. The mixed 2:1 complex  $[\text{KC}(\text{NbAs}_8)]^{1-}$  is present in the same spectrum that is presumably **2** capped by  $\text{K}^+$  on one side and  $\text{Cs}^+$  on the other. Interestingly, only the 1:1  $\text{Cs}-\text{NbAs}_8$  complex is observed in solution.

The  $[\text{KC}(\text{NbAs}_8)_2]^{1-}$  complex is also observed in the mass spectrum, which represents a dimer of **2** linked by alternating  $\text{K}^+$  and  $\text{Cs}^+$  ions. In this complex, the larger  $\text{Cs}^+$  ion is most likely in the capping position with  $\text{K}^+$  sandwiched between the two  $\text{NbAs}_8$  rings (Figure 5). This proposal is based on stacked guanosine complexes containing mixed  $\text{K}^+/\text{Cs}^+$  ions that show  $\text{K}^+$  in sandwich positions and  $\text{Cs}^+$  in the capping position.<sup>36</sup> In addition, the gas-phase studies of **2** only revealed a sandwich complex with  $\text{K}^+$  and not with  $\text{Cs}^+$ . For the solution  $[\text{CsNbAs}_8]^{2-}$  1:1 complex observed in the NMR experiments, the capping  $\text{Cs}^+$  is bound to 4 As atoms of the  $\text{As}_8$  ring on one side and most likely has  $\pi\text{-CH}_3\text{CN}$  ligands completing the coordination sphere.<sup>36–39</sup>

In contrast to the Group 6 analogues, all of the  $\text{NbE}_8$  complexes are diamagnetic. For electron-counting purposes, the  $\text{NbE}_8^{n-}$  ions can be considered as  $\text{E}_8^{8-}$  rings with  $\text{Nb}^{5+}$  ions in the Zintl–Klemm limit, which would give 16-electron,  $d^0$ -complexes. These electron counting principles are strictly formalisms and the actual charges on the transition metals are clearly quite different.<sup>35</sup> The structure and bonding of this class of complexes has been discussed in detail.<sup>35</sup> Further studies of this interesting series of compounds are currently in progress.

## Experimental Section

General operating procedures for our lab have been described previously.<sup>24</sup>  $\text{CsPh}_4\text{B}$  and  $\text{NaPh}_4\text{B}$  were purchased from Aldrich. Acetonitrile was purchased from Aldrich and distilled over calcium hydride and stored under nitrogen.  $\text{Nb}(\text{tol})_2$  was prepared according to published procedures.<sup>40</sup>

<sup>133</sup>Cs NMR spectra were recorded on a Bruker AM400 AVANCE spectrometer operating at 52.5 MHz. <sup>133</sup>Cs NMR data was referenced to 3.0 mM CsCl in  $\text{D}_2\text{O}$  (0 ppm). T1 values were determined by inversion recovery techniques and are 5 s and 10 ms for  $\text{CsPh}_4\text{B}$  and the complexed ion, respectively. A delay of 200 ms was used and the solutions were run in dry  $\text{CH}_3\text{CN}$ . A total of 5000 scans was collected for each spectrum. NMR samples were prepared from a 2.0 mM stock solution of  $\text{Cs}^+$ , which was prepared by dissolving 4.5 mg of  $\text{CsPh}_4\text{B}$  in 5.0 mL of  $\text{CH}_3\text{CN}$ . The concentration of  $[\text{NbAs}_8]^{3-}$  was varied. The stock solution was

prepared from the crystalline  $[\text{K}(2,2,2\text{-crypt})]_3[\text{NbAs}_8]$  in  $\text{CH}_3\text{CN}$ . A 0.50-mL aliquot from each solution was used to give a total of 1.0 mL of solution. To prepare a sample that contained equal amounts of free  $\text{Cs}^+$  and **2**, 3.9 mg of **2** was dissolved in 1.0 mL  $\text{CH}_3\text{CN}$ . A 0.50-mL aliquot of the 2.0 mM  $\text{Cs}^+$  solution was added to 0.50 mL of the solution of **2**. A 25 mM stock solution of  $\text{Na}^+$  was prepared by dissolving 43 mg of  $\text{NaPh}_4\text{B}$  in 5.0 mL of  $\text{CH}_3\text{CN}$  solution. A 0.20-mL portion of this solution was added into each NMR sample giving a total volume of 1.2 mL.

**$[\text{K}(2,2,2\text{-crypt})]_3[\text{NbAs}_8]\cdot\text{en}$** . In vial 1,  $\text{K}_3\text{As}_7$  (50.0 mg, 0.078 mmol) and 2,2,2-crypt (88.0 mg, 0.234 mmol) were dissolved in ca. 2 mL of en. In vial 2,  $\text{Nb}(\text{toluene})_2$  (21.6 mg, 0.078 mmol) was dissolved in toluene (ca. 1 mL), producing a red-brown solution. The contents of vial 2 were added to the contents of vial 1, yielding a dark brown solution. The reaction mixture was stirred for 8 h and filtered through tightly packed glass wool in a pipet. Toluene was added dropwise to the reaction mixture until precipitate formation was observed, and the solution was filtered immediately. Red crystals formed in the reaction vessel after 2 days. Yield: 19 mg (13%).

**$[\text{K}(2,2,2\text{-crypt})]_3[\text{NbSb}_8]$** . In vial 1,  $\text{K}_3\text{Sb}_7$  (50.0 mg, 0.052 mmol) and 2,2,2-crypt (58.2 mg, 0.156 mmol) were dissolved in ca. 2 mL of en. In vial 2,  $\text{Nb}(\text{toluene})_2$  (14.3 mg, 0.052 mmol) was dissolved in toluene (ca. 1 mL), producing a red-brown solution. The contents of vial 2 were added to the contents of vial 1, yielding a dark brown solution. The reaction mixture was stirred for 8 h and filtered through tightly packed glass wool in a pipet. Toluene was added dropwise to the reaction mixture until precipitate formation was observed, and the solution was filtered immediately. Red crystals formed in the reaction vessel after 2 days. Yield: 11 mg (9%).

## Crystallographic Studies

**$[\text{K}(2,2,2\text{-crypt})]_3[\text{NbAs}_8]\cdot\text{en}$** . A deep red block was mounted on a thin glass fiber using silicone grease and was then immediately placed under an  $\text{N}_2$  stream on a Siemens P4/PC diffractometer. The lattice parameters were optimized from a least-squares calculation on 32 carefully centered reflections of high Bragg angle. The data were collected using  $\omega$  scans with a  $1.0^\circ$  scan range. Three check reflections monitored every 97 reflections showed no systematic variation of intensities. Lattice determination and data collection were carried out using XSCANS software, version 2.10b. All data reduction, including Lorentz and polarization corrections, and structure solution and graphics were performed using SHELXTL.<sup>41</sup> The structure refinement was performed using SHELX 93.<sup>42</sup> The data were corrected for absorption (semiempirical, psi-scans) with max/min transmission factors of 0.807/0.628. Data collection parameters are given in Table 1.

The space group,  $P2_1/n$ , was uniquely determined from the systematic absences. The As, Nb, and K atoms were located from the direct methods solution (XS) whereas the C, O, and N atoms of the cryptands and solvate molecules were located from successive Fourier synthesis. All hydrogen atoms were fixed in positions of idealized geometry with C–H and N–H distances of 0.97 Å and were refined using the riding model in the HFIX facility in SHELXL 93. All nonhydrogen atoms were refined anisotropically in the final cycles. The refinement converged to  $R1 = 0.0509$  and  $wR2 = 0.0903$  for 6311  $F_o > 4\sigma(F_o)$ . The final difference map was essentially featureless with a few peaks ( $<0.66 \text{ e}\text{\AA}^{-3}$ ) near the carbon atoms of the en solvate.

(36) Forman, S. L.; Fetting, J. C.; Pieraccini, S.; Gottarelli, G.; Davis, J. T. *J. Am. Chem. Soc.* **2000**, *122*, 4060.

(37) Bryan, J. C.; Kavallieratos, K.; Sachleben, R. A. *Inorg. Chem.* **2000**, *39*, 1568.

(38) Werner, B.; Krauter, T.; Neumuller, B. *Organometallics* **1996**, *15*, 3746.

(39) Harrowfield, J. M.; Ogden, M. I.; Richmond, W. R.; White, A. H. *J. Chem. Soc., Chem. Commun.* **1991**, 1159.

(40) Cloke, F. G. N.; Green, M. L. H.; Price, D. H. *J. Chem. Soc., Chem. Commun.* **1978**, 431.

(41) Sheldrick, G. M. Siemens Analytical X-ray Instruments, Inc.: Madison, WI, 1994.

(42) Sheldrick, G. *Acta Crystallogr.* **1990**, *A46*, 467.

**[K(2,2,2-crypt)]<sub>3</sub>[NbSb<sub>8</sub>]**. A red plate with approximate orthogonal dimensions  $0.31 \times 0.12 \times 0.02 \text{ mm}^3$  was placed and optically centered on the Bruker SMART CCD system at  $-80 \text{ }^\circ\text{C}$ . The initial unit cell was indexed using a least-squares analysis of a random set of reflections collected from three series of  $0.3^\circ$  wide  $\omega$ -scans, 10 s per frame, and 25 frames per series that were well distributed in reciprocal space. Data frames were collected [Mo K $\alpha$ ] with  $0.3^\circ$  wide  $\omega$ -scans, 60 s per frame, and 606 frames per series. The crystal-to-detector distance was 4.494 cm, thus providing a nearly complete sphere of data to  $2\theta_{\text{max}} = 30.0^\circ$ . A total of 47 463 reflections were collected and corrected for Lorentz and polarization effects and absorption using Blessing's method as incorporated into the program SADABS with 10110 unique [R(int) = 0.0623].

The SHELXTL program package<sup>41</sup> was implemented to determine the probable space group and set up the initial files. System symmetry, systematic absences, and intensity statistics indicated the unique centrosymmetric monoclinic space group  $I2/a$ , a nonstandard setting of  $C2/c$  (no. 15). The structure was determined by direct methods with the successful location of the heavy atoms using the program XS, and the structure was refined with XL. A multitude of least-squares difference Fourier cycles were required to locate the remaining non-hydrogen atoms and sort out the various

disorders present. Non-hydrogen atoms were refined anisotropically whenever possible. Hydrogen atoms were placed in calculated positions. Because of the exceedingly weak data, they were truncated to  $2\theta_{\text{max}} = 30.0^\circ$  as indicated above. The final structure was refined to convergence [ $\Delta/\sigma \leq 0.001$ ] with R(F) = 12.86%, wR(F<sup>2</sup>) = 29.18%, GOF = 2.003 for all 10110 unique reflections [R(F) = 9.40%, wR(F<sup>2</sup>) = 25.61% for those 7603 data with  $F_o > 4\sigma(F_o)$ ]. The final difference Fourier map was featureless, indicating that the structure is both correct and complete. A summary of the crystallographic data is given in Table 1, but, due to the poor quality of the data, the corresponding bond distances and angles are not reported.

**Acknowledgment.** We are grateful to Prof. J. Davis for helpful comments and suggestions. We also thank Dr. S. Grumbine, Dr. J. Watkin, Dr. D. Clark, and Donna Gardner for assistance with the metal vapor synthesis at Los Alamos.

**Supporting Information Available:** Crystallographic files for **2** and **3** in cif format. This material is available free of charge via the Internet at <http://pubs.acs.org>.

IC035397X